ELSEVIER

Journal of Nuclear Materials 307–311 (2002) 95–99

journal of nuclear materials

www.elsevier.com/locate/jnucmat

Damage of structural materials for fusion devices under pulsed ion and high temperature plasma beams

V.N. Pimenov [a,*], E.V. Dyomina [a], L.I. Ivanov [a], S.A. Maslyaev [a], V.A. Gribkov [b], R. Miklaszewski [b], M. Scholz [b], A.V. Dubrovsky [c], I.V. Volobuev [c], Yu.E. Ugaste [d], F. Mezzetti [e], P. De Chiara [e], L. Pizzo [e], B. Kolman [f], A. Szydlowski [g]

[a] *A.A. Baikov Institute of Metallurgy and Material Science, RAS, Leninsky pr. 49, 117334 Moscow, Russia*
[b] *Institute of Plasma Physics and Laser Microfusion, Hery str. 23, 00-908 Warsaw, Poland*
[c] *P.N. Lebedev Physical Institute, RAS, Leninsky pr. 53, 117924 Moscow, Russia*
[d] *Pedagogical University of Tallinn, Narva Road 25, 10120 Tallinn, Estonia*
[e] *University of Ferrara, INPM, Via Paradiso 12, I-44100 Ferrara, Italy*
[f] *Institute of Plasma Physics ASCR, Za Slovankou 3, P.O. Box 17, 18221 Prague 8, Czech Republic*
[g] *The Andrzej Soltan Institute for Nuclear Studies, 05-400 Swierk by Warsaw, Poland*

Abstract

Results of experiments are presented on the influence of high-energy pulses on austenitic and ferritic steels carried out using dense plasma foci devices PF-1000 and PF-60 with hydrogen and deuterium as working gas, respectively. Pulsed irradiation of specimens was performed in two regimes: (1) under microsecond hydrogen plasma pulses with power density $q = 10^7$–10^9 W/cm^2, and (2) under 100-ns deuterium plasma pulses with $q = 10^9$–10^{11} W/cm^2. Features of damage, phase-structural transformations and compositional changes in these materials under these conditions were investigated.

1. Introduction

Dense plasma focus (DPF) installations, unlike other thermonuclear devices, have a number of important advantages [1–4]: (1) they provide an opportunity to expose materials to pulsed beams of various types (ion, electron, plasma, X-ray, neutron and shock waves) of high-power flux density (up to 10^{14} W/cm^2) with pulse duration in the range from 10^{-9} to 10^{-6} s; (2) they ensure an opportunity to vary the distribution of pulse energy between ion and plasma beams or change the sequence. The problem of plasma–surface interaction, in particular in pulsed thermonuclear installations, is especially amenable to the study of damage to materials under high-power energy pulses generated in DPF devices [5–9].

The aim of this study was to investigate the influence of pulsed ion beams and high temperature plasma, generated in DPF, on physical–chemical processes in austenitic chromium–manganese and ferritic steels. Similar steels have been tested under long low-power pulses because of their possible applications in TOKAMAK type thermonuclear reactors [10–14]. At present these steels are used inside the chambers of pulsed thermonuclear facilities and accelerators as structural materials.

The following specimens' properties were investigated: features of surface layer damage; thermal and radiation effects; structural and phase stability, and composition changes in surface layers.

* Corresponding author. Tel.: +7-095 135 9604; fax: +7-095 135 4540.
E-mail address: pimenov@ultra.imet.ac.ru (V.N. Pimenov).

0022-3115/02/$ - see front matter
PII: S0022-3115(02)00994-7

2. Experiment

2.1. Materials

The following materials were chosen for the experiments: austenitic chromium–manganese 25Cr12Mn20W and 10Cr12Mn20W steels as well as ferritic 10Cr9WV steel (see Table 1, composition in wt%). In this study the materials were melted and rolled to a thickness of 0.1 cm. Specimens were prepared as plates $1.5 \times 1.5 \times 0.1$ cm^3.

2.2. Experiments

The experiments were carried out using two different types of DPF devices: (1) PF-60, which has a Filippov-type (plane) electrode geometry [7], with deuterium as the working gas (initial pressure – 133 Pa); and (2) PF-1000, having Mather-type (cylindrical) electrodes [2,4], with hydrogen as the working gas (400 Pa).

Pulsed irradiation of specimens was performed at the cathode part of the DPF in two regimes: (1) by microsecond hydrogen plasma pulses with a power flux density $q = 10^7$–10^9 W/cm^2 (PF-1000), and (2) by 100-ns deuterium plasma pulses with $q = 10^9$–10^{11} W/cm^2 (PF-60). In each shot in the PF-60 device a specimen was irradiated first with a high-energy ion (with energy $E_i \geqslant 100$ keV) pulse and then, about 1 μs later, with the plasma jet. The energies of these two streams were approximately the same. In the case of the PF-1000 device the same fast ion beam (but having here a very low-energy content) hits the target about 6–8 μs earlier than the plasma jet, whereas the latter contributes the main part of the energy to the surface. The fluence of the fast ion beam acting on a test sample was determined by means of a CR-39 track detector [15], located close to the test sample.

3. Analysis methods

The irradiated samples were investigated by optical and scanning electron microscopy, X-ray diffraction analysis and X-ray spectral analysis. The comparative qualitative analysis of the carbon and oxygen distributions in the initial and irradiated specimens was carried out by means of local X-ray spectral analysis of the light elements [16].

4. Results

4.1. Deuterium ion beam and plasma jet influence

Under the test conditions, all materials were found to undergo surface melting and subsequent quenching, forming a specific droplet-ridge relief. When the number of the irradiation pulses N increased, the relief changed from random small structural elements (microdroplets) to larger ridges and valleys (in part directionally ordered).

Phase transformations in the austenitic steels were investigated previously [5]. It was shown that irradiation led to a $\gamma \rightarrow \alpha$ phase transformation in these steels. The volume fraction of α-phase increased with the number of pulses.

At the same time a monophase structure of α-ferrite was observed by X-ray diffraction analysis in both initial and irradiated ferritic 10Cr9WV steel specimens. This observation appeared to be independent of the number of pulses (for 5 or 20 pulses).

4.2. Hydrogen ion beam and plasma jet influence

For the austenitic chromium–manganese steels, it has been found that multiple microsecond pulse irradiation with power density $q \sim 10^7$–10^9 W/cm^2 results in evaporation, melting and quenching of the surface layer. The irradiated materials typically exhibit a wavelike surface.

The nature of the damage for steels with 0.25% C and 0.10% C was different. In the first case craters were observed on the surface, while in the second case mainly blisters were seen. A SEM picture of the irradiated surface of the 25CrMn20W steel specimen is presented in Fig. 1. As seen, the surface irradiated with 3 pulses shows a significant quantity of deep craters with diameters (∅) up to about 10 μm, small blisters (∅ ⩽ 1 μm), and microcracks. Most of the craters are situated on the

Table 1
Chemical content of investigated steels

Steel	Elements (mass%)									
	C	Cr	Mn	Si	W	Ta	V	P	S	N
10Cr12Mn20W	0.10	12.10	20.10	0.02	2.05	–	–	0.02	0.02	0.01
25Cr12Mn20W	0.25	11.57	20.75	0.02	2.01	–	0.1	0.04	0.008	0.003
10Cr9WV	0.11	9.2	0.65	0.3	1.0	0.1	0.15	0.02	0.007	0.036

convex parts of the surface. In contrast the 10Cr12Mn20W steel surface showed a different damage character (see Fig. 2). There are a substantial number of large blisters ($\varnothing \leqslant 10$ μm) and craters. For the austenitic steels the number of defects per unit area ρ has been determined. The results are presented in Table 2. The surface density of defects ρ formed during a pulse was in the range of $0.67–1.00 \times 10^5$ cm^{-2}.

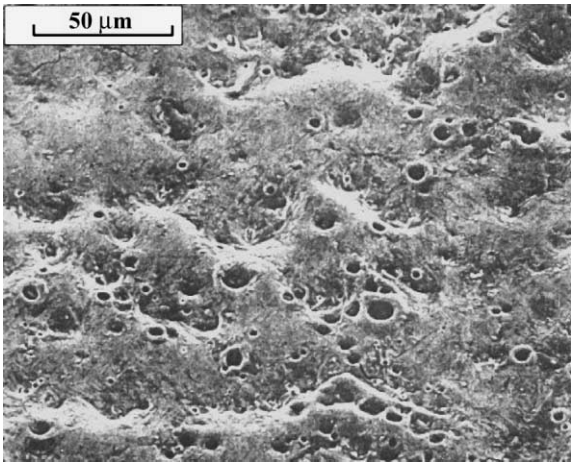

Fig. 1. Surface of the 25Cr12Mn20W steel after 3 hydrogen plasma pulses in the PF-1000 device.

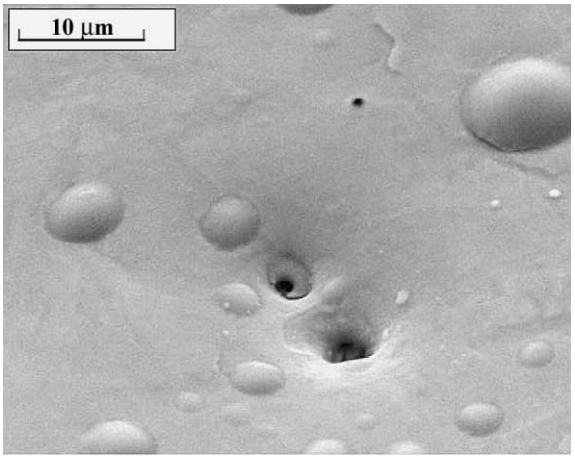

Fig. 2. Surface of the 10Cr12Mn20W steel after 8 hydrogen plasma pulses in the PF-1000 device.

The order of magnitude for the observed values of ρ is in good agreement with the dose ρ_i of hydrogen ions having energy $E_i \geqslant 100$ keV, which were implanted in irradiated specimens during a pulse. This dose magnitude ρ_i was determined by means of a track detector [15]. In other words, for the irradiation regime investigated the macroscopic surface density of structure defects (blisters and craters) correlates with the fluence of high-energy hydrogen ions implanted into specimen per relevant pulse. The value of this density was about 10^5 cm^{-2}.

Distribution of elements before and after irradiation was analyzed qualitatively. The distributions of Fe, Mn and Cr in the initial state of a specimen of the 10Cr12Mn20W steel were uniform. But after 3 pulses of irradiation a redistribution of the components was observed (see Fig. 3). Where blisters occurred, a significant increase in Mn content and a reduction in Fe content took place. After 6 pulses this effect remained but was less evident.

Quantitative analysis of the chemical composition of 10Cr12Mn20W steel was performed for the original steel and after 10 pulses of irradiation. The following results were obtained (in at.%): original surface – Al (<0.104); Si (0.779); Cr (11.735); Mn (20.083); Fe (66.874); Cu (<0.357); W (<0.333); irradiated specimen – Al (0.536); Si (0.227); Cr (11.181); Mn (17.388); Fe (66.610); Cu (3.471); W (0.588). Some reduction of Mn content and increase of Cu content were observed.

Carbon and oxygen distributions were studied in both types of austenitic steels. After irradiation the distributions were less smooth, unlike the relatively uniform distribution in the original surface. Peaks on the curves of oxygen and carbon distributions across the surfaces, found in the austenitic steel specimens after 3 hydrogen plasma pulses, corresponded to convex parts of the irradiated surface where craters and blisters formed. A correlation was also observed between the two curves: that is, an increase in carbon content was accompanied by an increase in the oxygen content.

Table 2
Density of structure defects on surface of austenitic steels after irradiation in PF-1000 device

#	Material	The main kind of defects	The number of pulses	Surface density of defects ρ (10^5 cm^{-2})
1	25Cr12Mn20W ($L = 70$ cm)	Craters	3	2.0
2	25Cr12Mn20W	Craters	3	3.0
3	10Cr12Mn20W	Blisters	6	5.3
4	10Cr12Mn20W	Blisters, craters	8	6.2

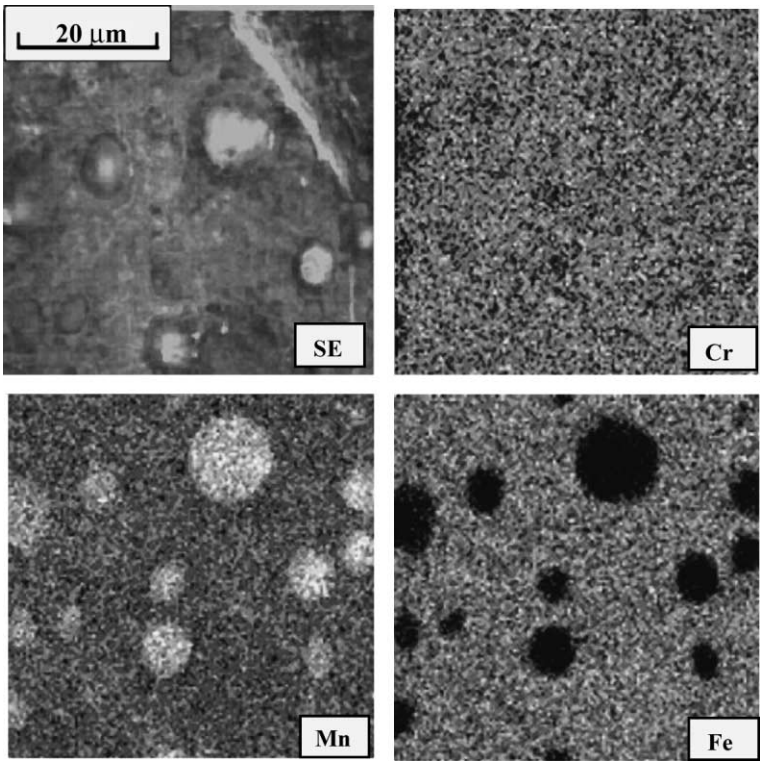

Fig. 3. Secondary electron image (SE) and distribution of characteristic X-ray radiation for Fe, Cr and Mn on the surface of 10Cr12Mn20W steel after 3 hydrogen plasma pulses in the PF-1000 device.

5. Discussion

The observed $\gamma \rightarrow \alpha$ phase transformation in austenitic steels under powerful pulses of radiation [5] is probably connected with preferential evaporation of Mn. This is confirmed by results of quantitative analysis of chemical composition of steel 10Cr12Mn20W after hydrogen ion and plasma multipulse irradiation. After 10 pulses at $q = 10^7$–10^9 W/cm^2, the concentration of Mn in the surface was reduced by approximately 2.7%. Increasing q by two orders of magnitude (in experiments in PF-60 in comparison with the experiments in PF-1000) exacerbated this effect and resulted in intense reduction of Mn content in the irradiated surface layer. Since Mn stabilizes the γ-phase in austenitic steels [17], its selective evaporation leads to decomposition of the γ-phase and precipitation of the α-phase during crystallization of the melted surface layer. The phase composition of manganese-free ferritic steels did not change after multipulse irradiation, while a crystallization texture $(200)_\alpha$ along the temperature gradient was observed.

In experiments on the PF-60 device, the thickness d of the evaporated layer was close to the projected range R in the steel for ions with energy $E_i \geqslant 100$ keV. So the damage of the irradiated material was mainly thermal. In experiments on PF-1000, when the power flux density q was significantly less and d was less than R, the implantation of high-energy hydrogen ions into the target material occurred. Correlation between the density of macroscopic surface defects and the density (fluence) of the high-energy hydrogen ions shows that implanted ions influenced the formation of the surface defects (craters and blisters) in the steel (see Figs. 1 and 2). Taking into account the results of element analysis (Fig. 3) it appears that implanted hydrogen ions have created vacancy clusters [18,19]. This cluster appears to act as a nucleus of a gas phase (micropore) and hence a sink for atoms of the light elements. Under the subsequent (6–8 μs later on) heating by the plasma jet [4], Mn as well as compounds of light elements CO, CO_2 may have collected in these micropores, with formation and growth of gas bubbles. After crystallization and cooling these bubbles (blisters) burst with the formation of craters (see Fig. 1) or were trapped in the solid state (see Fig. 2). Manganese from the retained gas phase, as well as compounds of carbon and oxygen, condensed onto the inner surface of the blisters. That may be why an increase of manganese as well as carbon and oxygen content in the vicinity of blisters and

craters was observed on the surface of the irradiated steels.

An increase in the Cu content in the irradiated steel 10Cr12Mn20W is related to the deposition of copper on the irradiated specimen due to an evaporation of the copper anode of the PF-1000 device [2,4].

6. Conclusion

The main forms of damage and structural changes in austenitic and ferritic steels, irradiated by pulsed streams of fast ions and hydrogen or deuterium plasmas, were determined. Phase stability of ferritic steel and $\gamma \rightarrow \alpha$ phase transformation in austenitic steels were found. It was shown that in the regime of the irradiation realized at the PF-1000 installation, blisters were mainly formed at the irradiated surface of the austenitic steel with 0.1% C; whereas in the steel with 0.25% C, predominantly craters formed. It was found that the surface density of macroscopic structural defects (blisters and craters) were determined by the fluence of high-energy ($E_i \geqslant 100$ keV) hydrogen ions implanted into a specimen. It is proposed that the formation of the surface bubbles is connected with a process of evaporation of volatile components of the steels from a liquid phase into micropores created by hydrogen ions implantation.

Acknowledgements

This work is supported in part by INCO-COPERNICUS (contract # ERB IC 15-CT98-0811), International Atomic Energy Agency (contract # 11943) and FOP 'Integration' (Project # A – 098/2001).

References

[1] V.A. Gribkov, J. Moscow Phys. Soc. 3 (3) (1993) 321.
[2] M. Scholz, R. Miklaszewski, V.A. Gribkov, F. Mezzetti, Nukleonika 45 (3) (2000) 155.
[3] A.V. Dubrovsky, V.A. Gribkov, Nukleonika 45 (3) (2000) 159.
[4] M. Borowetski, P. De Chiara, V.A. Gribkov, A.V. Dubrovsky, E.V. Dyomina, L.I. Ivanov, S.A. Maslyaev, F. Mezzetti, V.N. Pimenov, L. Pizzo, M. Scholz, A. Szydlowski, Y.E. Ugaste, I.V. Volobuev, Nukleonika 46 (Suppl. 1) (2001) 117.
[5] L.I. Ivanov, V.N. Pimenov, S.A. Maslyaev, E.V. Dyomina, V.A. Gribkov, F. Mezzetti, P. De Chiara, L. Pizzo, Nukleonika 45 (3) (2000) 203.
[6] L.I. Ivanov, V.N. Pimenov, Ü. Ugaste, E.V. Dyomina, S.A. Maslyaev, V.A. Gribkov, F. Mezzetti, Def. Dif. Forum 194–199 (2001) 1093.
[7] S.A. Maslyaev, V.N. Pimenov, Yu.M. Platov, E.V. Dyomina, S.Ya. Betsofen, V.A. Gribkov, A.V. Dubrovsky, Perspektiv. Mater. (Adv. Mater.) 3 (1998) 39 (in Russian).
[8] J. Feugeas, G. Grigioni, G. Sanchez, A. Rodrigues, Surf. Eng. 14 (1) (1998) 62.
[9] A.V. Dubrovsky, V.A. Gribkov, Yu.P. Ivanov, P. Lee, S. Lee, M. Liu, V.A. Samarin, Nukleonika 46 (Suppl. 1) (2001) 107.
[10] F. Abe, F.A. Garner, H. Kayano, J. Nucl. Mater. 212–215 (1994) 760.
[11] R.L. Klueh, E.A. Kenik, J. Nucl. Mater. 212–215 (1994) 437.
[12] S. Ohnuki, H. Takahashi, H. Kinoshita, S. Mochizuki, J. Nucl. Mater. 212–215 (1994) 755.
[13] N.P. Lyakishev, V.Ya. Dashevsky, E.V. Dyomina, L.I. Ivanov, Yu.M. Platov, M.D. Prusakova, V.P. Kolotov, M.V. Alenina, J. Nucl. Mater. 258–263 (1998) 1300.
[14] L.I. Ivanov, S.A. Maslyaev, V.N. Pimenov, E.V. Dyomina, Yu.M. Platov, J. Nucl. Mater. 271&272 (1999) 405.
[15] M. Sadowski, E.M. Al-Mashhadani, A. Szydlowski, et al., Nucl. Instrum. and Meth. B 86 (1994) 311.
[16] A.I. Kozlenkov, Y.I. Belov, V.G. Bogdanov, A.I. Shulgin, in: Proceedings of the 5th Microprobe Conference, Leipzig, 1981, p. 47.
[17] A.V. Vertkov, V.A. Evtichin, I.E. Lyublinski, A.A. Syichev, E.V. Demina, M.D. Prusakova, J. Nucl. Mater. 203 (1993) 158.
[18] V.T. Zabolotnyi, V.M. Lazorenko, Phys. Chem. Mater. Treat. 3 (1993) 17.
[19] V.T. Zabolotnyi, L.I. Ivanov, A.L. Suvorov, Phys. Chem. Mater. Treat. 2 (1994) 5.